

# No differences in radiological changes after 3D conformal vs VMAT-based stereotactic radiotherapy for early stage non-small cell lung cancer

© 2017 The Authors. Published by the British Institute of Radiology

[Serena Badellino](#), MD<sup>1</sup>, , [Jacopo Di Muzio](#) MD<sup>1</sup>, , [Giulia Schivazappa](#), MD<sup>2</sup>, , [Alessia Guarneri](#), MD<sup>1</sup>, , [Riccardo Ragona](#), MSc<sup>1</sup>, , [Sara Bartoncini](#), MD<sup>1</sup>, [Elisabetta Trino](#), MD<sup>1</sup>, , [Andrea Riccardo Filippi](#), MD<sup>1</sup>, , [Paolo Fonio](#), MD<sup>2</sup>, , [Umberto Ricardi](#), MD<sup>1</sup>,

<sup>1</sup>Department of Oncology, Radiation Oncology, University of Torino, Torino, Italy

<sup>2</sup>Department of Surgical Sciences, Radiology, University of Torino, Torino, Italy

<https://doi.org/10.1259/bjr.20170143>

Received: February 28, 2017

Accepted: July 18, 2017

Published Online: September 04, 2017

## Objective:

To compare patterns of acute and late radiological lung injury following either 3D conformal or image-guided volumetric modulated arc therapy stereotactic radiotherapy for Stage I non-small-cell lung cancer.

## Methods:

We included 148 patients from a prospective mono-institutional stereotactic body radiation therapy (SBRT) series (time interval 2004–2014), treated with prescription BED<sub>10 Gy</sub> (at 80%) in the range 100–120 Gy. The first 95 patients (2004–2010) were planned with 3D-CRT, with a stereotactic body frame. The second cohort (2010–2014) included 53 patients, planned with volumetric IMRT on a smaller planning target volume generated from a patient's specific internal target volume, with a frameless approach through cone-beam CT guidance. Acute and late radiological modifications were scored based on modified Kimura's and Koenig's classifications, respectively.

## Results:

Median follow-up time was 20.5 months. The incidence of acute radiological changes was superimposable between the groups: increased density was observed in 68.4 and 64.2% of patients for 3D-CRT and VMAT, respectively, and patchy ground glass opacity in 23.7 and 24.5%, respectively; diffuse ground glass opacity was 2.6 vs 9.4%, respectively, and patchy consolidation 2.6 vs 1.9%, respectively. Late changes occurred in approximately 60% of patients: modified conventional pattern was the most frequent modification (25 vs 32.6%, respectively); other patterns were less common (mass-like 19.6 vs 17.4%, and scar-like 13 vs 10.9%, respectively).

## Conclusion:

Results of the present study indicate that the pattern of radiological lung changes following SBRT for peripheral early stage non-small-cell lung cancer is not influenced by the different techniques used for planning and delivery.

## Advances in knowledge:

This comparative observational study shows that smaller margins, image guidance and most importantly dose distribution do not change the pattern of radiological injury after lung SBRT; the same scoring system can be used, and expected incidence is similar.

Stereotactic body radiation therapy (SBRT) is currently the standard option in patients with Stage I non-small cell lung cancer (NSCLC) who are unfit or refuse surgery.<sup>1–6</sup> Technological progresses have expanded treatment options, for example through the introduction of techniques such as volumetric modulated arc therapy (VMAT) as an alternative to multiple non-coplanar 3D-CRT

fields arrangement.<sup>7</sup> The purpose of VMAT is to quickly deliver highly conformal dose, by contemporaneously enabling dose escalation with greater sparing of normal tissues.<sup>8,9</sup> In addition, the association of this technique with motion management strategies such as respiratory gating and/or four-dimensional CT (4DCT) and image-guided radiation therapy further reduces the risk of geographical miss and spares unnecessary irradiation of normal lung.<sup>10</sup> Due to the differences in dose distribution, it is reasonable to expect that VMAT will result in different radiological patterns of radiation-induced lung injuries in comparison with conventional 3D-CRT. Initial data are available on the differential pattern of lung injury among different SBRT techniques, and aim of this study was to compare acute and late radiological lung changes following either 3D or image-guided VMAT stereotactic radiotherapy for Stage I NSCLC.<sup>11</sup>

## Methods and Materials

From 2004 to 2014, 148 patients were included in this observational study. Eligibility criteria for SBRT were (a) contraindication to surgery after multidisciplinary evaluation, (b) ECOG performance status  $\leq 2$ , (c) accurate staging, with positron emission tomography and brain CT scan and (d) no prior thoracic radiation therapy. In the absence of histological diagnosis, a new and/or increasing lung nodule, with abnormal 18FDG uptake, was considered as malignant. The entire cohort of patients was divided in 2 groups according to the technique used for SBRT delivery. The first group of 95 patients (time interval 2004–2014) was planned with 3D-CRT, while the second group of 53 patients (time interval 2010–2014) was planned with VMAT. All patients had peripheral tumours and a prescription BED<sub>10 Gy</sub> (at 80%-isodose) in the range 100–120 Gy.

Patients in Group 1 were immobilized in the supine position with a stereotactic body frame (Elekta Oncology Systems, Stockholm, Sweden) with a diaphragm compression device to reduce tumour motion. The gross tumour volume corresponded to the clinical target volume and was outlined in sequential axial CT images using a CT lung window setting (166–400 Hounsfield units). The clinical target volume-planning target volume margins were 5 mm in antero-posterior and latero-lateral directions and 10 mm in cranio-caudal direction for setup errors and organ motion. Treatment was delivered with an Elekta Precise Linear Accelerator (Elekta Oncology Systems, Stockholm, Sweden), using multiple non-coplanar shaped fields, with 6 to 10 MV photons and positioning verification with Portal Images (EPID).

For patients in Group 2, a frameless approach was used, with Blue Bag vacuum pillow (Elekta Oncology Systems, Stockholm, Sweden) shaped on each patient's body and the use of cone-beam CT image-guidance prior to any fraction. A 4D-CT scan with breath monitoring was performed and an internal target volume was defined in which the GTV included the tumour position in all phases of respiratory cycle, outlined using a CT windows setting. A margin of 3 mm in each direction was added to the internal target volume in order to create the PTV. Monaco software (Elekta Oncology Systems, Stockholm, Sweden) was used for treatment planning and a Monte Carlo algorithm for dose calculation. Single or multiple VMAT arcs were used, delivered with an Elekta Axes TM Linear Accelerator (Elekta, Stockholm, Sweden), with 6–10 MV photons. Figure 1 illustrates two typical examples of the dose distribution achieved with either 3D-CRT or VMAT plans.

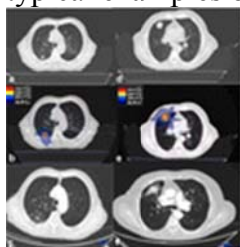


**Figure 1.** On the left, a case of a 75-year patient with Stage IA NSCLC, 45 Gy/3 fractions, treated with 3D-CRT; (a) CT scan pre-treatment, (b) planning CT scan with isodoses (c) CT scan 6 months after the procedure. On the right, a case of an 82-year patient with Stage IB NSCLC, 45 Gy/3 fractions, treated with VMAT; (d) CT scan before treatment; (e) planning

**CT scan with isodoses; (f) CT scan 6 months after SBRT. SBRT, stereotactic body radiation therapy; VMAT, volumetric modulated arc therapy.**

Ninety-five percent of the PTV was encompassed by the 80% prescription isodose, for both 3D-CRT and VMAT plans. Average  $D_{\max}$  for 3D-CRT was 105% (acceptable range 103–110%) and for VMAT 104% (acceptable range 102–109%).

Ipsilateral Mean Lung Dose (in 2 Gy equivalent,  $MLD_2$ ) was calculated for each patient (radiation pneumonitis,  $a/b = 3$  Gy);<sup>12</sup> constraints for thoracic organs at risk were derived from the American Association of Physicists in Medicine Task Group 101 recommendation.<sup>13</sup>

Patients in the two groups underwent a first diagnostic total body CT with intravenous contrast after 2 months from the completion of RT treatment. Subsequent CT scans had an interval of 3 months for the first 2 years. For the study purposes, all CT scans have been assessed by two trained physicians (a radiation oncologist and pulmonary radiologist) in order to assess the occurrence and grade of any toxicity. The observers were not blinded with respect to the radiation technique used. Acute changes (<6 months from SBRT) were scored according to the five-point scoring system modified from Kimura et al<sup>14</sup> (1 = diffuse consolidation, 2 = patchy consolidation, 3 = diffuse “ground glass opacity” (GGO), 4 = patchy “ground glass opacity”, 5 = no changes).<sup>15</sup> Late changes (>6 months post SBRT) were scored using Koenig’s Scale (0 = absence of changes, 1 = modified conventional pattern, 2 = mass like pattern, 3 = scar like pattern).<sup>16</sup> Clinical lung toxicity was recorded from our prospectively collected observational database, and was graded using the RTOG score for both acute and late (occurring after 6 months) events (<http://www.rtog.org/members/toxicity>).

In order to test the difference in the distribution of patient characteristics, we performed the Student’s t test (mean difference for continuous variables) or, when indicated, the Fisher’s exact test (proportional difference for categorical variables).

## Results

Patient characteristics are summarized in Table 1. Lesions were smaller in the 3D-CRT vs VMAT group (82 vs 56.6% Stage IA and 17.9 vs 43.4% Stage IB tumours, respectively,  $p = 0.02$ ). Mean tumour diameter was 2.5 vs 3 cm ( $p = 0.01$ ), while PTV was 35.1 cc (range 7.7–101 cc) vs 40.3 cc (range 7.3–75 cc) ( $p = 0.03$ ), respectively. In the 3D-CRT group, a larger proportion of patients had PS ECOG 1 (49.9%), in comparison with the VMAT group (24.5%,  $p = 0.01$ ). Dosimetric parameters were comparable.

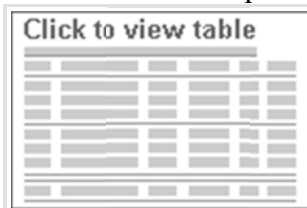


**Table 1. Patients’ and treatment characteristics**

**Table 1. Patients’ and treatment characteristics**

	3D-CRT (n = 95)		VMAT (n = 53)		p (Student’s t-test)	p (Fisher’s test)
	N°	%	N°	%		
<b>Gender</b>						0.53
Male	77	81	40	75.5		
Female	18	19	13	24.5		
<b>Age at treatment (mean, range)</b>	75	(53–89)	76	(52–88)	0.31	
<b>PS (ECOG)</b>						0.01

	3D-CRT (n = 95)		VMAT (n = 53)		p (Student's t-test)	t-p (Fisher's test)
	N°	%	N°	%		
0	48	50.1	40	75.5		
1	47	49.9	13	24.5		
<b>Histology</b>						0.68
Unknown	48	50.5	24	45.3		
Squamous cell carcinoma	16	16.8	9	17		
Adenocarcinoma	19	20	16	30.2		
Others	12	12.7	4	7.5		
<b>Stage</b>						0.02
IA	78	82.1	30	56.6		
IB	17	17.9	23	43.4		
<b>Diameter in cm (mean, range)</b>	2.5 (1–5)		3 (1.3–5)		0.01	
<b>PTV in cc (mean, range)</b>	35.1 (7.7–101)		40.3 (7.3–75)		0.03	
<b>BED (mean, range)</b>	110.8 100–120		110.5 100–120		0.38	
<b>Dose and fractionation</b>						
15 Gy × 3 fx	82	86	9	16		NR
14 Gy × 3 fx	12	13	2	3		NR
11 Gy × 5 fx	1	1	21	39		NR
7.5 Gy × 8 fx	0	0	21	39		NR
<b>MLD<sub>2Gy</sub>ipsi (mean, range)</b>	11.7 (4–28)		10.4 (4–17.2)		0.32	
<b>MLD<sub>2Gy</sub>con (mean, range)</b>	2.9 (1.1–5)		3.1 (1.8–5)		0.4	
<b>MLD<sub>2Gy</sub>bil (mean, range)</b>	9.5 (6.6–17)		7 (4.5–11)		0.3	
<b>V20 ipsi (mean, range)</b>	13.8 (11–19)		15.6 (10–22)		0.5	
<b>V10 ipsi (mean, range)</b>	21 (18–29)		24.6 (17–31.8)		0.2	
<b>V5 ipsi (mean, range)</b>	33 (27–38)		35 (26.5–40)		0.3	
<b>V20 bil (mean, range)</b>	8 (6.9–12)		7.8 (5–13)		0.8	
<b>V10 bil (mean, range)</b>	14 (11–17.9)		14.4 (12.9–19)		0.8	
<b>V5 bil (mean, range)</b>	24.6 (21–29)		24.8 (20–30.1)		0.8	
<b>V5 con (mean, range)</b>	14 (11.7–19.9)		15.1 (11–19)		0.3	

3D-CRT, three-dimensional conformal radiotherapy); BED, biologically effective dose; Bil, bilateral; Con, contralateral; Fx, fractions; Gy, gray; Ipsi, Ipsilateral; con, contralateral; bil, bilateral; MLD, mean lung dose; NR, not reported; PTV, planning target volume; PS ECOG, performance status according to Eastern Cooperative Oncology Group; VMAT, volumetric modulated arc therapy;

Median follow up time was 20.5 months. According to the modified Kimura's classification, the incidence of acute radiological injury was superimposable between the groups: no evidence of

increased density was observed in 68.4 vs 64.2% of patients for 3D-CRT and VMAT, respectively; patchy GGO in 23.7 vs 24.5%, respectively; a low proportion of other acute modifications, such as diffuse GGO (2.6 vs 9.4%) and patchy consolidation (2.6 vs 1.9%), was recorded; diffuse consolidation pattern was only observed in 3D-CRT patients (2.6%). All differences were not statistically significant (Pearson's chi-squared  $p = 0.55$ ).

Late changes occurred in approximately 60% of patients: modified conventional pattern was the most frequent modification (25 vs 32.6% for 3D-CRT vs VMAT, respectively), while other patterns were less common (mass-like pattern 19.6 vs 17.4%, and scar-like pattern 13 vs 10.9%, respectively). All differences were again not statistically significant (Pearson's chi-squared  $p = 0.82$ ). Complete data showing the distribution of acute and late radiological changes frequency per group are reported in Figures 2 and 3.

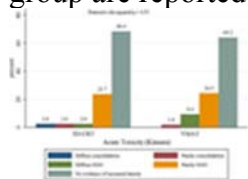


Figure 2. Distribution of acute radiological changes according to the five-point scoring system modified from Kimura et al<sup>15</sup> GGO, ground glass opacity.

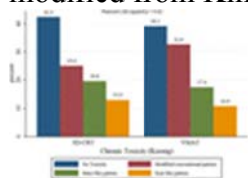


Figure 3. Distribution of late radiological changes, scored by Koenig's Scale.

Concerning clinical toxicity, most of patients did not experience neither acute nor late toxicity; we observed only 2.1 and 3.8% RTOG acute Grade  $\geq 3$  radiation pneumonitis, respectively, and no substantial differences were found between VMAT and 3D-CRT.

## Discussion

Since SBRT has become a viable alternative to surgery for Stage I NSCLC, the interpretation of post-treatment radiological findings acquired increased importance. The definition of local control is today purely based on radiological findings, and both radiologists and radiation oncologists should be able to recognize heterogeneous CT appearances at different time-points. The differential diagnosis between progression, no response or intra and/or peri-tumoral radiation-induced lung injury is particularly challenging, and the use of different radiotherapy techniques, such as VMAT and 3D-CRT, might influence observations and lead to different results. In our study, we compared the radiological findings of two different planning/delivery techniques in order to recognize possible differences in radiological toxicity profiles. Patients treated with VMAT seem to be more unfavourably selected for some characteristics (for example, a higher proportion of Stage IB tumours); conversely, a larger fraction of PS ECOG 0 patients was observed. These slightly unbalanced features reflect the progressive changes in clinical indications over time (a higher proportion of patients with larger tumours were judged eligible for SBRT, and the number of patients who refused surgery in the VMAT group was increased). However, the distribution of radiological changes (acute and late) resulted substantially superimposable (Figures 2 and 3). It is possible that the higher proportion of “modified conventional pattern” observed for VMAT (32.6 vs 25%, respectively, despite not significant) might reflect the prevalence of larger tumours in this group: at this regard, a higher sample would possibly have confirmed a trend towards the onset of specific density changes according to tumour volumes.

In general, the incidence and grade of late radiological changes reported by the present study were quite similar to other reports. Aoki et al analysed a cohort of 31 patients (48 Gy/4 fractions with 3D-CRT): most of them (26%) had a slightly increased density of the treated area at CT scans within the first 6 months followed by patchy consolidation as the second most frequent pattern



(21%), while a minority demonstrated a discrete (6%) or solid consolidation (0%).<sup>17</sup> Trovò et al reported on 68 patients treated with SBRT over a period of 18 months. Between 2 and 6 months (acute radiological toxicity), the CT pattern was distributed as follows: patchy consolidation in 33% of patients and diffuse consolidation pattern in 27%, whereas patchy GGO occurred in only the 6% of patients. With regards to late toxicity (beyond 6 months) the authors found 11 patients (44%) with a modified conventional pattern, 7 patients (28%) with mass-like pattern, 4 patients (16%) with a scar-like pattern and only 3 patients (12%) with no changes.<sup>18</sup> Senthil et al firstly suggested that the differences between the different radiological patterns might be related to the different technique used and consequent dose distribution.<sup>19</sup> In a previous report by Palma et al, lung density progressively increased after a cumulative dose of 6 Gy, with an apparent plateau after 40 Gy.<sup>15</sup> The pattern of radiological toxicity could also be influenced by other clinical factors, as chronic obstructive pulmonary disease (COPD) or emphysema.<sup>14,15</sup>

The main data series on radiological changes according to different planning techniques for lung SBRT, Rapid Arc (RA) and 3D-CRT, comes from Palma et al.<sup>11</sup> The Authors analysed a homogeneous cohort of 75 Stage I patients, 25 planned with RA and 50 with 3D-CRT. As in our study, they used a risk adapted fractionation strategy with total doses ranging from 54 to 60 Gy in 3 fractions for peripheral lesions, 55 Gy and 60 Gy in 5 fractions for lesions in broad contact with the chest wall and 60 Gy in 8 fractions for lesions nearby bronchial tree and brachial plexus (all prescribed at 80% isodose). Acute radiological toxicity was classified according to the five-point scoring system modified from Kimura et al.<sup>14</sup> Similarly to our study, no differences were observed, with a prevalence of “no increased density” or consolidative radiological changes in both groups (40% in 3D-CRT patients and 36% in RA patients). In a sequent study, again Palma et al analysed the correlation between ipsilateral CT density changes and SBRT dose in 50 Stage I NSCLC, reporting density modifications in the low dose regions (<10 Gy) and more evident changes at doses > 20 Gy, with a plateau at higher doses.<sup>15</sup> CT density changes were also strongly associated with increasing PTV volumes, as a result of increased volumes of irradiated normal lung. Arcangeli et al analysed the pattern of radiological injury in 28 elderly patients (31 lesions) affected by NSCLC Stage I, treated with Helical Tomotherapy-based SBRT, with an average PTV of 47.3 cm<sup>3</sup>, a BED greater than 100 Gy (71%) and a risk-adapted fractionation. They found no acute radiological changes in 80% of cases while other radiological findings were equally distributed among other categories (6.5% patchy GGO, 6.5% patchy consolidation, 6.5% diffuse consolidation). In contrast with our findings, the most frequent chronic radiological pattern was mass-like (16%), followed by modified conventional (12%) and scar-like (12%).<sup>20</sup>

Strengths of our study are the quite large sample size and the homogeneity of the two analyzed cohorts (in terms of median age, gender, histology and SBRT dose); moreover, we used the same follow-up protocol for all patients, assessing all images together with a radiologist. Limitations includes the absence of a matched-paired analysis between the groups, that are unbalanced for stage (82.1 vs 56.6% for Stage IA and 17.9 vs 43.4% for Stage IB) and PTV, reflecting the different time interval where 3D-CRT and VMAT were used, together with potential unknown biases in treatment selection. However, these limitations should not have a substantial impact on the main study purpose, focused on radiological changes according to the technique used for SBRT planning and delivery.

## Conclusion

According to the present observational study, the use of 3D-CRT or VMAT for lung SBRT for early stage lung cancer has no influence on the pattern of acute and late pulmonary radiological changes detected at follow-up CT scans.

## References

1. Vansteenkiste J, Crinò L, Doooms C, Douillard JY, Faivre-Finn C, Lim E, et al. 2nd ESMO

- consensus conference on lung cancer: early-stage non-small-cell lung cancer consensus on diagnosis, treatment and follow-up. *Ann Oncol* 2014; **25**: 1462–74.[10.1093/annonc/mdu089](#) [Crossref](#), [Medline](#), [ISI](#), [Google Scholar](#)
2. Xia T, Li H, Sun Q, Wang Y, Fan N, Yu Y, et al. Promising clinical outcome of stereotactic body radiation therapy for patients with inoperable stage I/II non-small-cell lung cancer. *Int J Radiat Oncol Biol Phys* 2006; **66**: 117–25.[10.1016/j.ijrobp.2006.04.013](#) [Crossref](#), [Medline](#), [ISI](#), [Google Scholar](#)
  3. Baumann P, Nyman J, Hoyer M, Wennberg B, Gagliardi G, Lax I, et al. Outcome in a prospective phase II trial of medically inoperable stage I non-small-cell lung cancer patients treated with stereotactic body radiotherapy. *J Clin Oncol* 2009; **27**: 3290–6.[10.1200/JCO.2008.21.5681](#) [Crossref](#), [Medline](#), [ISI](#), [Google Scholar](#)
  4. Timmerman R, Paulus R, Galvin J, Michalski J, Straube W, Bradley J, et al. Stereotactic body radiation therapy for inoperable early stage lung cancer. *JAMA* 2010; **303**: 1070–6.[10.1001/jama.2010.261](#) [Crossref](#), [Medline](#), [ISI](#), [Google Scholar](#)
  5. Chang JY, Balter PA, Dong L, Yang Q, Liao Z, Jeter M, et al. Stereotactic body radiation therapy in centrally and superiorly located stage I or isolated recurrent non-small-cell lung cancer. *Int J Radiat Oncol Biol Phys* 2008; **72**: 967–71.[10.1016/j.ijrobp.2008.08.001](#) [Crossref](#), [Medline](#), [ISI](#), [Google Scholar](#)
  6. Ricardi U, Frezza G, Filippi AR, Badellino S, Levis M, Navarria P, et al. Stereotactic ablative radiotherapy for stage I histologically proven non-small cell lung cancer: an Italian multicenter observational study. *Lung Cancer* 2014; **84**: 248–53.[10.1016/j.lungcan.2014.02.015](#) [Crossref](#), [Medline](#), [ISI](#), [Google Scholar](#)
  7. Huo M, Gorayski P, Pinkham MB, Lehman M. Advances in radiotherapy technology for non-small cell lung cancer: what every general practitioner should know. *Aust Fam Physician* 2016; **45**: 805–9. [Medline](#), [ISI](#), [Google Scholar](#)
  8. Mackie TR, Balog J, Ruchala K, Shepard D, Aldridge S, Fitchard E, et al. Tomotherapy. *Semin Radiat Oncol* 1999; **9**: 108–17.[10.1016/S1053-4296\(99\)80058-7](#) [Crossref](#), [Medline](#), [ISI](#), [Google Scholar](#)
  9. Arcangeli S, Agolli L, Portalone L, Migliorino MR, Lopergolo MG, Monaco A, et al. Patterns of CT lung injury and toxicity after stereotactic radiotherapy delivered with helical tomotherapy in early stage medically inoperable NSCLC. *Br J Radiol* 2015; **88**: 20140728.[10.1259/bjr.20140728](#) [Link](#), [ISI](#), [Google Scholar](#)
  10. Slotman BJ, Lagerwaard FJ, Senan S. 4D imaging for target definition in stereotactic radiotherapy for lung cancer. *Acta Oncol* 2006; **45**: 966–72.[10.1080/02841860600902817](#) [Crossref](#), [Medline](#), [ISI](#), [Google Scholar](#)
  11. Palma DA, Senan S, Haasbeek CJ, Verbakel WF, Vincent A, Lagerwaard F. Radiological and clinical pneumonitis after stereotactic lung radiotherapy: a matched analysis of three-dimensional conformal and volumetric-modulated arc therapy techniques. *Int J Radiat Oncol Biol Phys* 2011; **80**: 506–13.[10.1016/j.ijrobp.2010.02.032](#) [Crossref](#), [Medline](#), [ISI](#), [Google Scholar](#)
  12. Ricardi U, Filippi AR, Guarneri A, Giglioli FR, Mantovani C, Fiandra C, et al. Dosimetric predictors of radiation-induced lung injury in stereotactic body radiation therapy. *Acta Oncol* 2009; **48**: 571–7.[10.1080/02841860802520821](#) [Crossref](#), [Medline](#), [ISI](#), [Google Scholar](#)
  13. Benedict SH, Yenice KM, Followill D, Galvin JM, Hinson W, Kavanagh B, et al. Stereotactic body radiation therapy: the report of AAPM Task Group 101. *Med Phys* 2010; **37**: 4078–101.[10.1118/1.3438081](#) [Crossref](#), [Medline](#), [ISI](#), [Google Scholar](#)
  14. Kimura T, Matsuura K, Murakami Y, Hashimoto Y, Kenjo M, Kaneyasu Y, et al. CT appearance of radiation injury of the lung and clinical symptoms after stereotactic body

- radiation therapy (SBRT) for lung cancers: Are patients with pulmonary emphysema also candidates for SBRT for lung cancers? *Int J Radiat Oncol Biol Phys* 2006; **66**: 483–91.[10.1016/j.ijrobp.2006.05.008](#) [Crossref](#), [Medline](#), [ISI](#), [Google Scholar](#)
15. Palma DA, van Sörnsen de Koste J, Verbakel WF, Vincent A, Senan S. Lung density changes after stereotactic radiotherapy: a quantitative analysis in 50 patients. *Int J Radiat Oncol Biol Phys* 2011; **81**: 974–8.[10.1016/j.ijrobp.2010.07.025](#) [Crossref](#), [Medline](#), [ISI](#), [Google Scholar](#)
  16. Koenig TR, Munden RF, Erasmus JJ, Sabloff BS, Gladish GW, Komaki R, et al. Radiation injury of the lung after three-dimensional conformal radiation therapy. *AJR Am J Roentgenol* 2002; **178**: 1383–8.[10.2214/ajr.178.6.1781383](#) [Crossref](#), [Medline](#), [ISI](#), [Google Scholar](#)
  17. Aoki T, Nagata Y, Negoro Y, Takayama K, Mizowaki T, Kokubo M, et al. Evaluation of lung injury after three-dimensional conformal stereotactic radiation therapy for solitary lung tumors: CT appearance. *Radiology* 2004; **230**: 101–8.[10.1148/radiol.2301021226](#) [Crossref](#), [Medline](#), [ISI](#), [Google Scholar](#)
  18. Trovo M, Linda A, El Naqa I, Javidan-Nejad C, Bradley J. Early and late lung radiographic injury following stereotactic body radiation therapy (SBRT). *Lung Cancer* 2010; **69**: 77–85.[10.1016/j.lungcan.2009.09.006](#) [Crossref](#), [Medline](#), [ISI](#), [Google Scholar](#)
  19. Senthil S, Dahele M, van de Ven PM, Slotman BJ, Senan S. Late radiologic changes after stereotactic ablative radiotherapy for early stage lung cancer: a comparison of fixed-beam versus arc delivery techniques. *Radiother Oncol* 2013; **109**: 77–81.[10.1016/j.radonc.2013.08.034](#) [Crossref](#), [Medline](#), [ISI](#), [Google Scholar](#)
  20. Arcangeli S, Agolli L, Portalone L, Migliorino MR, Lopercolo MG, Monaco A, et al. Patterns of CT lung injury and toxicity after stereotactic radiotherapy delivered with helical tomotherapy in early stage medically inoperable NSCLC. *Br J Radiol* 2015; **88**: 20140728.[10.1259/bjr.20140728](#) [Link](#), [ISI](#), [Google Scholar](#)